Geochemistry, Geophysics, Geosystems

Supporting Information for

The influence of lithospheric thickness variations beneath Australia on seismic anisotropy and mantle flow

C.M. Eakin [1*], D.R. Davies [1], S. Ghelichkhan [1], J.P. O'Donnell [2†], S. Agrawal [1]

[1] Research School of Earth Sciences, The Australian National University, Canberra, ACT, Australia

[2] Geological Survey of South Australia, Department for Energy and Mining, Adelaide, SA, Australia

*Corresponding author: Caroline M. Eakin (caroline.eakin@anu.edu.au)

† Now at Geological Survey of Western Australia, Perth, WA, Australia

Contents of this file

Additional Supporting Information (Files uploaded separately)

Introduction

This supporting information provides additional text regarding quality control of the measurements (ST1), further context regarding the results of previous studies (ST2), and added justification for an interpretation in terms of a single layer of anisotropy (ST3). Ten additional supplemental figures are also provided that may be of interest to the reader.

Text ST1. Methodology: Quality control criteria for **KS* splitting measurements

For a split (i.e. non-null) measurement to be of acceptable quality this was visually identified in several ways (see Figure S1a). Firstly, the shear-wave pulse should be clearly visible on both the radial and transverse components that is distinct from the background noise. Secondly, the pulse shape should be similar on the fast/slow components. Thirdly, the uncorrected particle motion is expected to be elliptical but becomes linear and aligned with the back-azimuth upon correction. Additional quantitative indicators include errors of less than 1 second in δt and $< 22.5°$ in Φ at the 95% confidence level. Individual results from both the RC and SC methods were expected to agree within similar error magnitudes (Wüstefeld and Bokelmann, 2007).

Null measurements, which indicate the shear-wave has not undergone splitting, are also subject to similar quality control criteria (refer to Figure S1b). This includes a clearly visible shear-wave pulse on the radial component but minimal or no energy on the transverse component. This should equate to linear uncorrected particle motion that is aligned with the source-receiver back-azimuth. Additionally null measurements tend to display a large discrepancy in apparent delay times between the two methods, with RC values approaching zero while the SC method can take any value.

Text ST2. Discussion: Is seismic anisotropy beneath Australia coherent or weak?

Unlike the earliest studies of SKS splitting in Australia, our results demonstrate clear shear-wave splitting patterns that vary regionally but are spatially consistent within a given province, such as across the Gawler Craton. There are several possible reasons for the emergence of this clear pattern. Most earlier studies that reported weak splitting and complex anisotropy beneath Australia were limited by a relatively small number of (<35) stations, sometimes sparsely distributed over the continent, and often with relatively short recording spans of less than a year (Clitheroe and van der Hilst, 1998; Heintz and Kennett, 2006, 2005; Özalaybey and Chen, 1999; Vinnik et al., 1992). Over time the Australian National Seismograph Network has created a dataset of long-running permanent stations with now more than ten years of data at most sites. Recent studies that utilize these long-running stations (Ba et al., 2023; Birkey and Ford, 2022; Eakin et al., 2021) have been increasingly converging towards consistent shear-wave splitting patterns across Australia that was not possible to resolve previously with the limited datasets available.

Shear-wave splitting studies in Australia are also restricted by the limited back-azimuthal coverage for SKS in this part of the world (Figure 2b). We found that the inclusion of the PKS phase, which uses events in a different epicentral distance range to SKS, helped to expand the number of and backazimuthal range of usable events. We also found that focusing on a smaller number of but higher quality stacked results was helpful in revealing the underlying spatial splitting patterns. With temporary stations that only operate for short periods (e.g. 6-18 months), in Australia these may only return 1 or 2 split measurements that may be strongly back-azimuthally dependent. As outlined further in section ST3 below, variations in fast-direction of up 45° are known to occur as a function of back-azimuth simply due to systematic measurement error (Eakin et al., 2019). Stacking of the measurements helped to negate these back-azimuthal variations due to systematic error (Figures S9-10) and thus reveal consistent regional trends.

It is also typical in Australian shear-wave splitting studies to retrieve more null results (i.e. shear-waves that have not undergone splitting) at a given station than split results. This still holds true in this study (Figure S3). As first noted by (Eakin et al., 2021), this is likely attributable to the unfortunate alignment of the inferred fast/slow axes of anisotropy over large swaths of the continent and the narrow back-azimuthal range of events (140°-160°) that dominates *KS splitting analyses for this region (Figure 2b and S4). Less prolific splitting and a higher frequency of nulls reported in Australia may therefore still be consistent with coherent anisotropy, rather than weak anisotropy and/or precise multi-layering to generate apparent isotropy (e.g. Heintz and Kennett, 2006; Özalaybey and Chen, 1999).

Text ST3. Discussion: Interpretation in terms of a single anisotropic layer

The method we have employed involves stacking individual error matrices to determine the best-fit values for the splitting parameters (Φ and δt) at each station. This inherently assumes that the shear-wave splitting from each station is best explained by a flat-lying single-layer of anisotropy. Evidence from surface wave studies of azimuthal anisotropy would suggest however that this may not be the case (Debayle et al., 2005; Debayle and Kennett, 2000; Fishwick et al., 2008; Simons et al., 2002). Such studies tend to show strong anisotropy aligned N-S with the plate motion at the base of the plate ~ 200-250 km depth. The azimuthal anisotropy tends to be weaker at shallower lithospheric depths (e.g. 50-150 km) with shorter-scale lateral variations of the fast axis orientation, often attributed to complex tectonic histories and deformational fabrics preserved within the lithosphere (e.g. Figure S7).

Evidence for two or more layers of anisotropy is usually assessed from *KS splitting by studying the variation of splitting parameters with back-azimuth (which is equivalent to the initial polarization for core-refracted phases) (Rümpker and Silver, 1998; Silver and Savage, 1994). For temporary stations with only a handful of results each this is impractical, but it is possible to assess back-azimuthal variations at the long-running ANSN permanent stations (Figure S10).

An illustrative example is shown in Figure S9 for station AU:OOD located in the vicinity of the Lake Eyre Basin array (Figure 2). In most cases these permanent stations display a clear 90° periodicity in the splitting parameters with back-azimuth. Most notably a rotation of the fast direction (Φ) with back-azimuth can be seen that closely follows a 45° slope, i.e. Φ = backazimuth ± 45°, as represented by the red line in Figure S9. This stark pattern is consistent with a known systematic error in splitting measurements (Monteiller and Chevrot, 2010; Vecsey et al., 2008; Wüstefeld and Bokelmann, 2007) and has been previously observed for stations in Australia (Eakin et al., 2021). Importantly, it is fundamentally not possible to reproduce this trend by modelling two-layers of anisotropy, as demonstrated in Eakin et al., (2019). It is however easily predictable. Simple models of this systematic error based on the station stacked-average splitting parameters reproduce well the back-azimuthal variance of the results (Figures S9-S10). This suggests that our method of stacking is valid, as the stacked values are consistent with the expected back-azimuthal variation for a single layer of anisotropy. This however does not imply that multiple layers of anisotropy cannot exist, but rather that they are not required to explain the data.

(a) Example of a Split

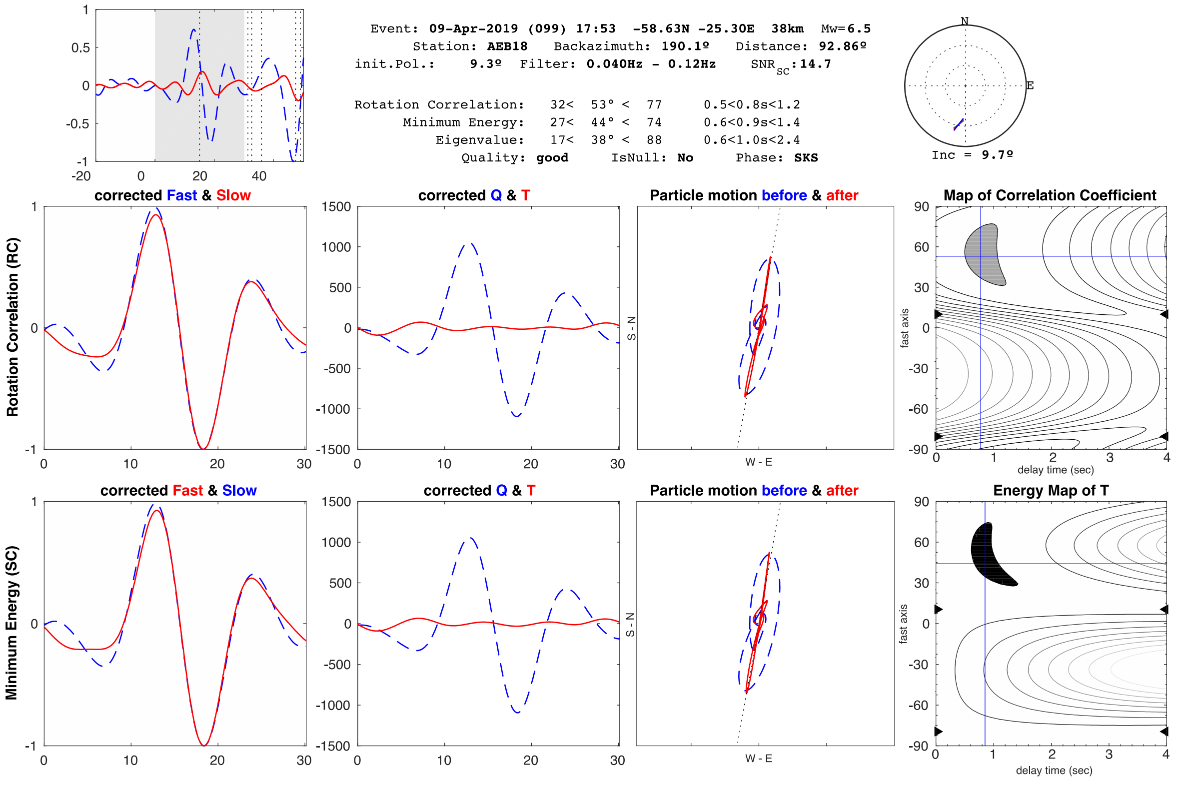

(b) Example of a Null

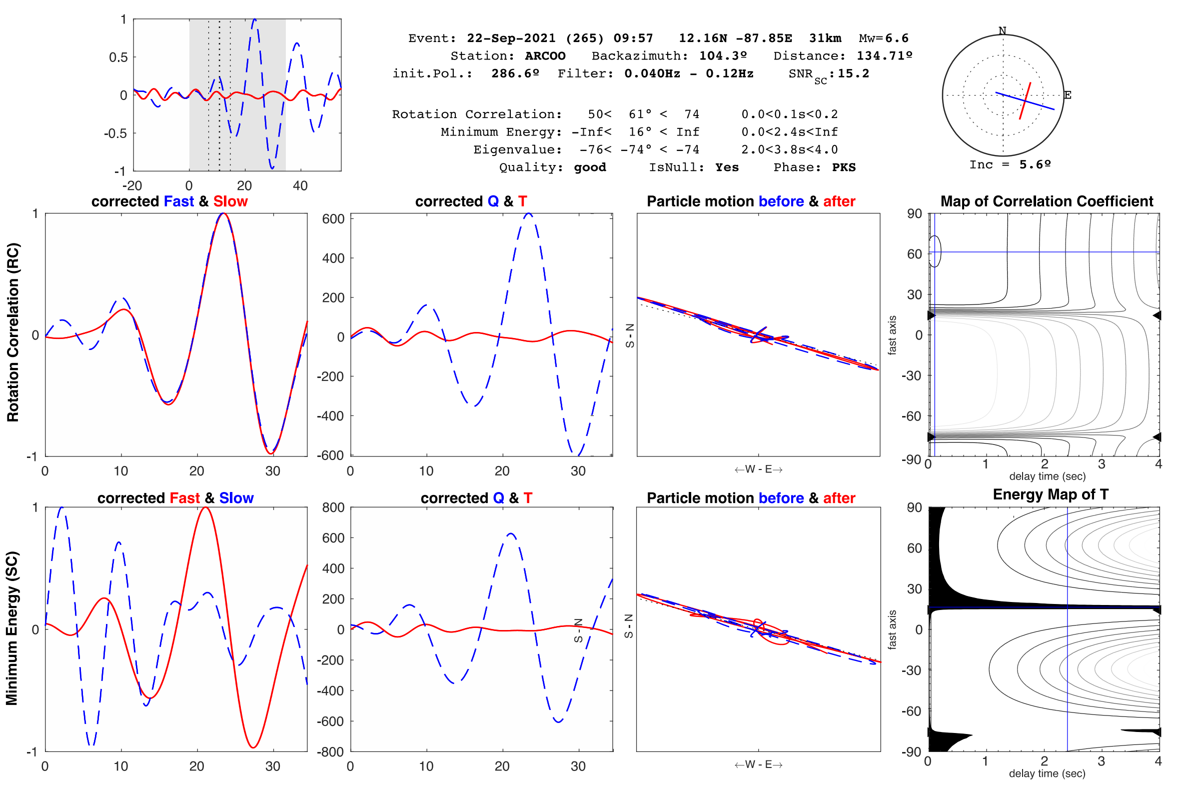

Figure S1. Example of the diagnostic plots generated by the SplitLab user interface (Wüstefeld et al., 2008) for (a) a split measurement at station AEB18 from the Lake Eyre Basin (5G) network, and (b) a null measurement at station ARCOO from the AusArray-SA (6K) network. For the split measurement shown in (a), the SplitLab output demonstrates a clear *KS pulse above the noise on both the transverse (T) and radial (Q) components (upper left plot). The waveform shape is similar for the corrected fast and slow components (1st column). *KS energy is removed on the corrected transverse component showing low amplitudes (2nd column). The particle motion shows initial elliptical motion, which is corrected, to linear motion aligned with the backazimuth, i.e. the dotted black line (3rd column). The error matrices show similar best-fit solutions for both the RC and SC methods and relatively small 95% confidence intervals, i.e. black/grey shaded region (4th column). The example shown in (b) demonstrates the features that are characteristic for a null, that is a shear-wave that has not undergone any splitting. A clear *KS pulse above the noise is seen on the radial (Q) component but not the transverse (T) (upper left plot). The initial particle motion in blue is linear and aligned with the backazimuth (3rd column). The error matrix for the RC method predicts close to zero delay time and a fast direction which is orientated 45° from the backazimuth (4th column). In contrast the error matrix for the SC method displays a classic ‘pronged’ type pattern lined up with the backazimuth ±90°.

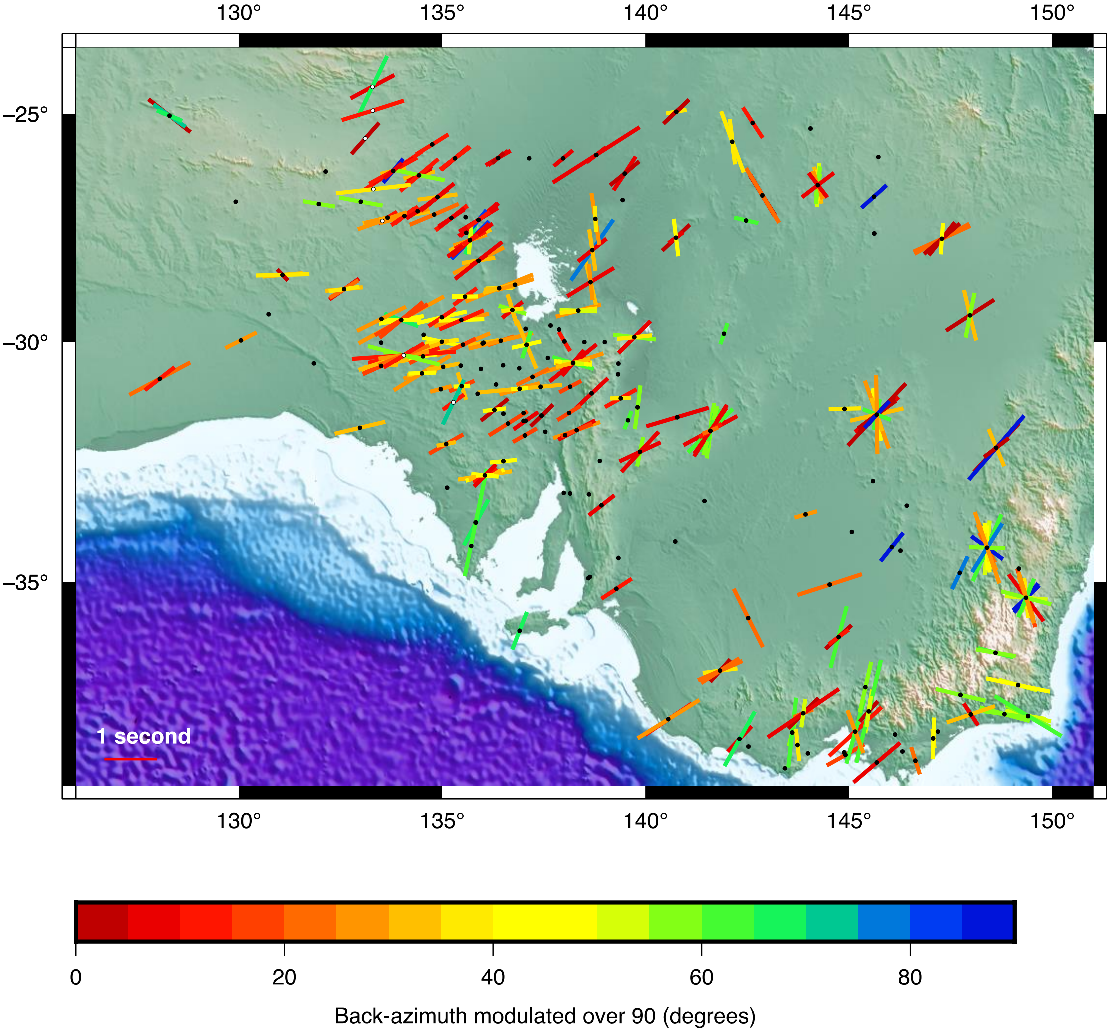

Figure S2. All 367 individual *KS split measurements recorded at 118 stations across the study region. The fast direction is reflected by the orientation of the bar, and the delay time by its length. The bars are coloured by the back-azimuth of the raypath, modulated over 90°, to reflect any periodic patterns with backazimuth.

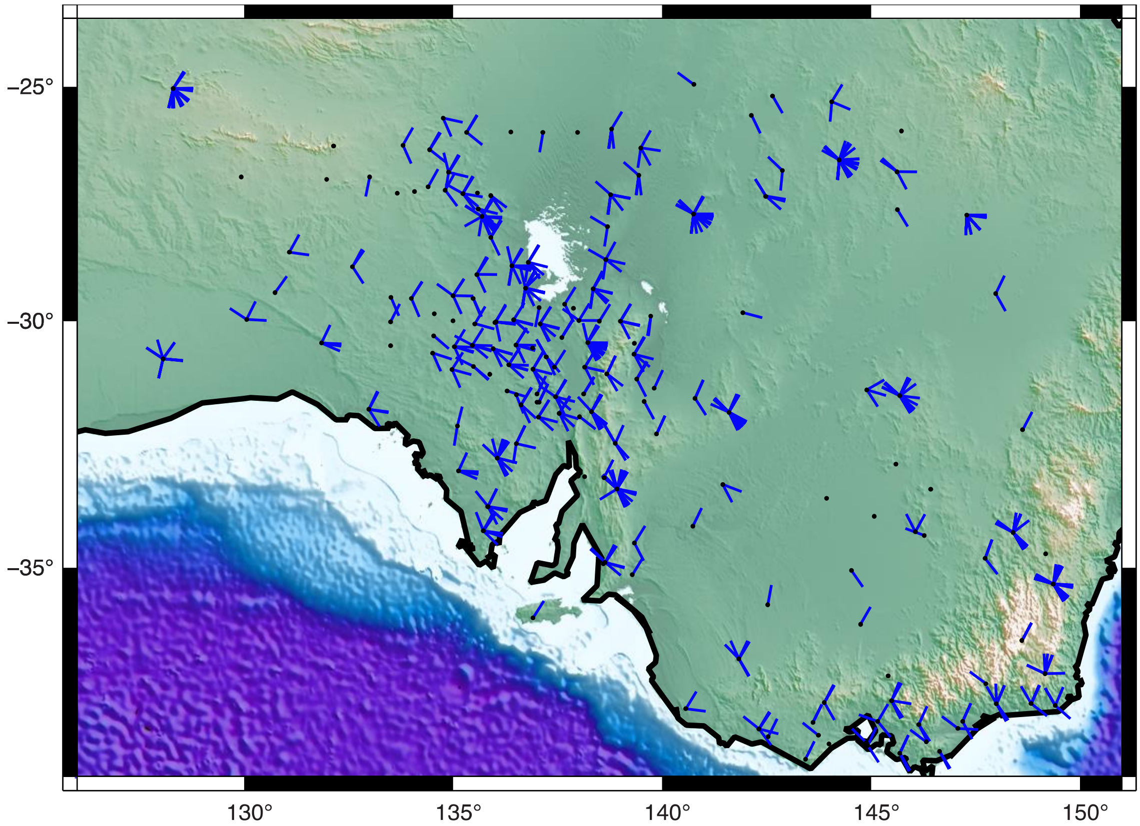

Figure S3. All 840 individual null measurements recorded across 157 stations. Each blue tick represents one measurement, pointing in the direction of the event back-azimuth at which the null was recorded

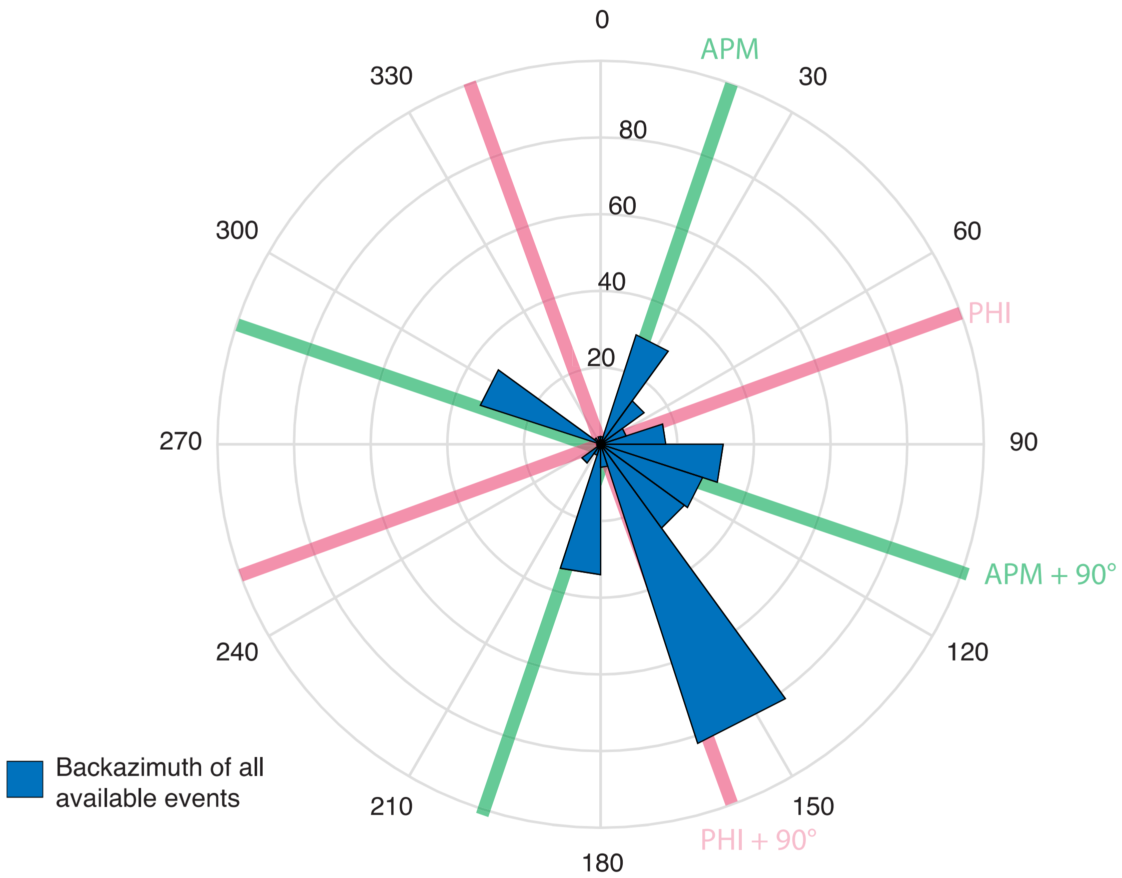

Figure S4. Rose plot showing the back-azimuthal availability of events for station OOD, same as Figure 2b. The majority of events (>80) fall within the 144° -162° back-azimuthal bin, which overlaps with the inferred slow axis of anisotropy for this region labelled 'PHI + 90°' in pink. The inferred fast axis is also shown in pink (labelled 'PHI') based on the average fast direction over the Galwer Craton (Φ = 70°). For comparison, the approximate orientation of the absolute plate motion (APM) for this region is also shown in green. If the inferred slow/fast axes of anisotropy align with the APM, as is seen for stations in eastern Australia (Figure 3), then these would overlap with most of the secondary events available at NNE, ESE, SSW, and WNW azimuths. The overlap between the availability of events, and the inferred slow/fast axes, likely contributes to the difficulty in recording clear shear-wave splitting measurements in Australia, as well as the relatively large number of null results (e.g. Figure S3).

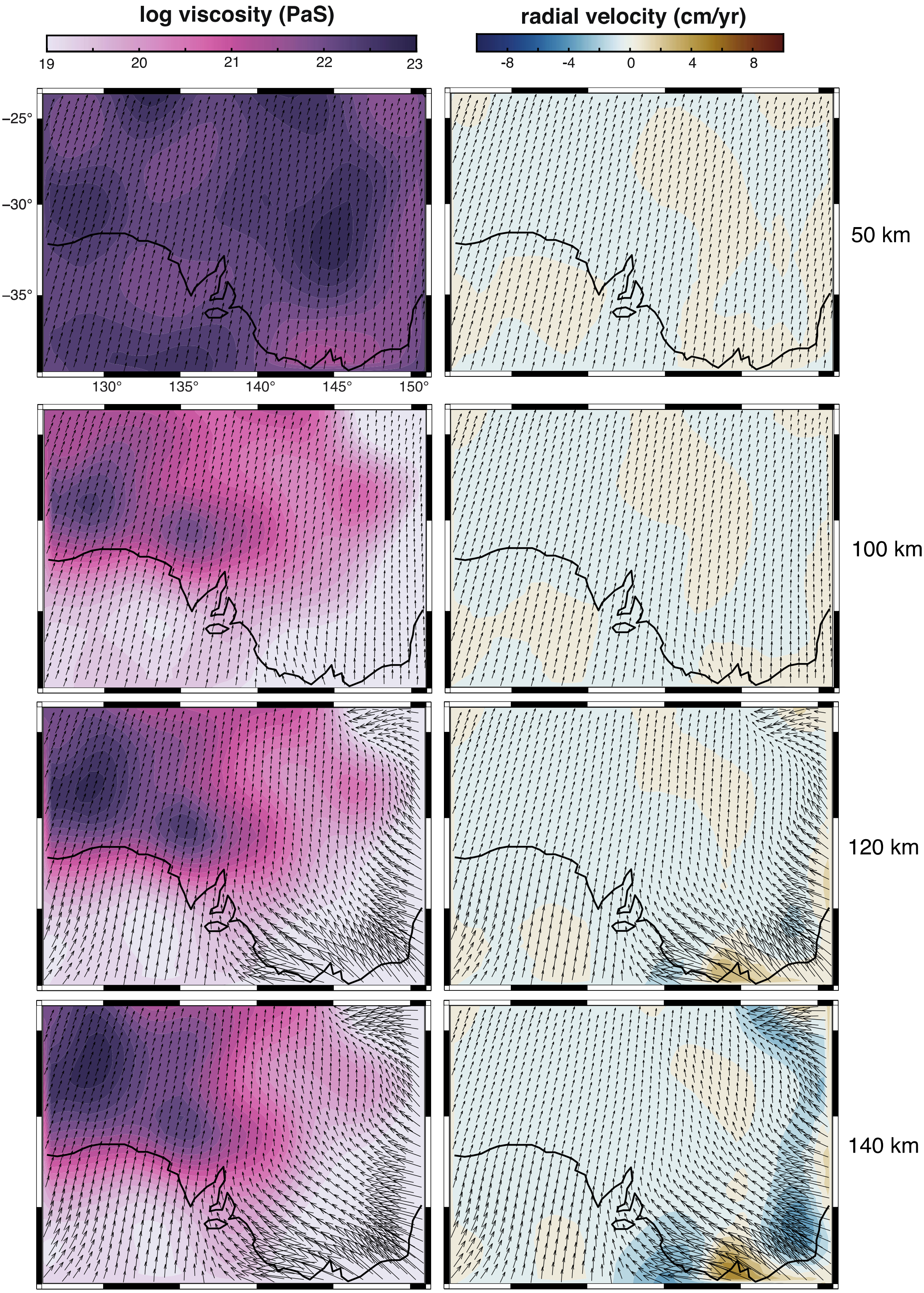

log viscosity (PaS)
19
20
21
22
23
radial velocity (cm/yr)
-8
-4
0
4
8
−25°
−30°
−35°
130°
135°
140°
145°
150°
50 km
100 km
120 km
140 km

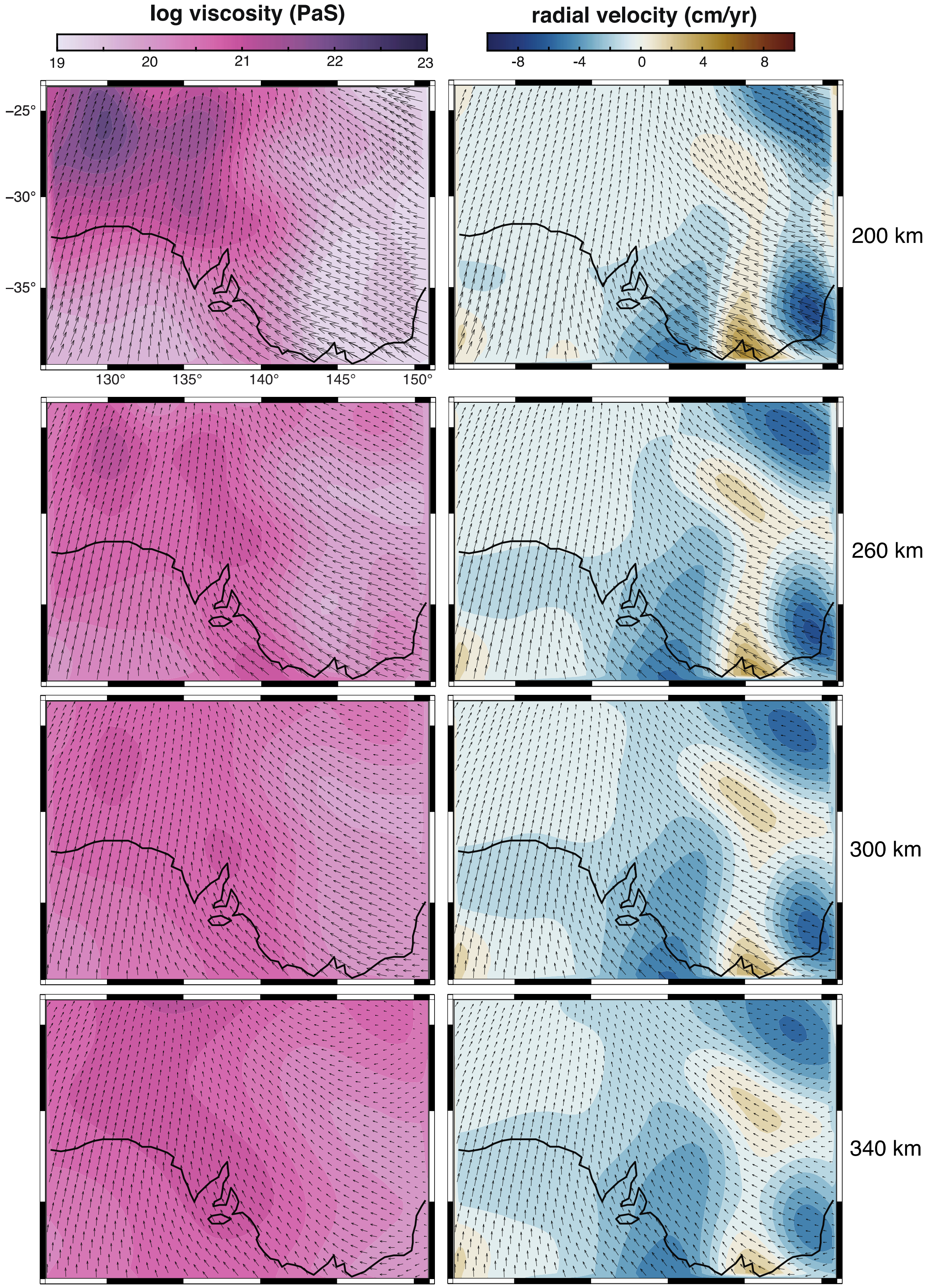

Figure S5. Upper-mantle depth slices through our mantle flow simulation (same as Figure 5). The left hand column illustrates the inferred mantle viscosity at the various depths. The right hand column background colours show the radial component of the velocity field, with red colours indicating upwelling and blue colours indicating down-welling. The small black arrows in all plots indicate the direction of the tangential component of the velocity field.

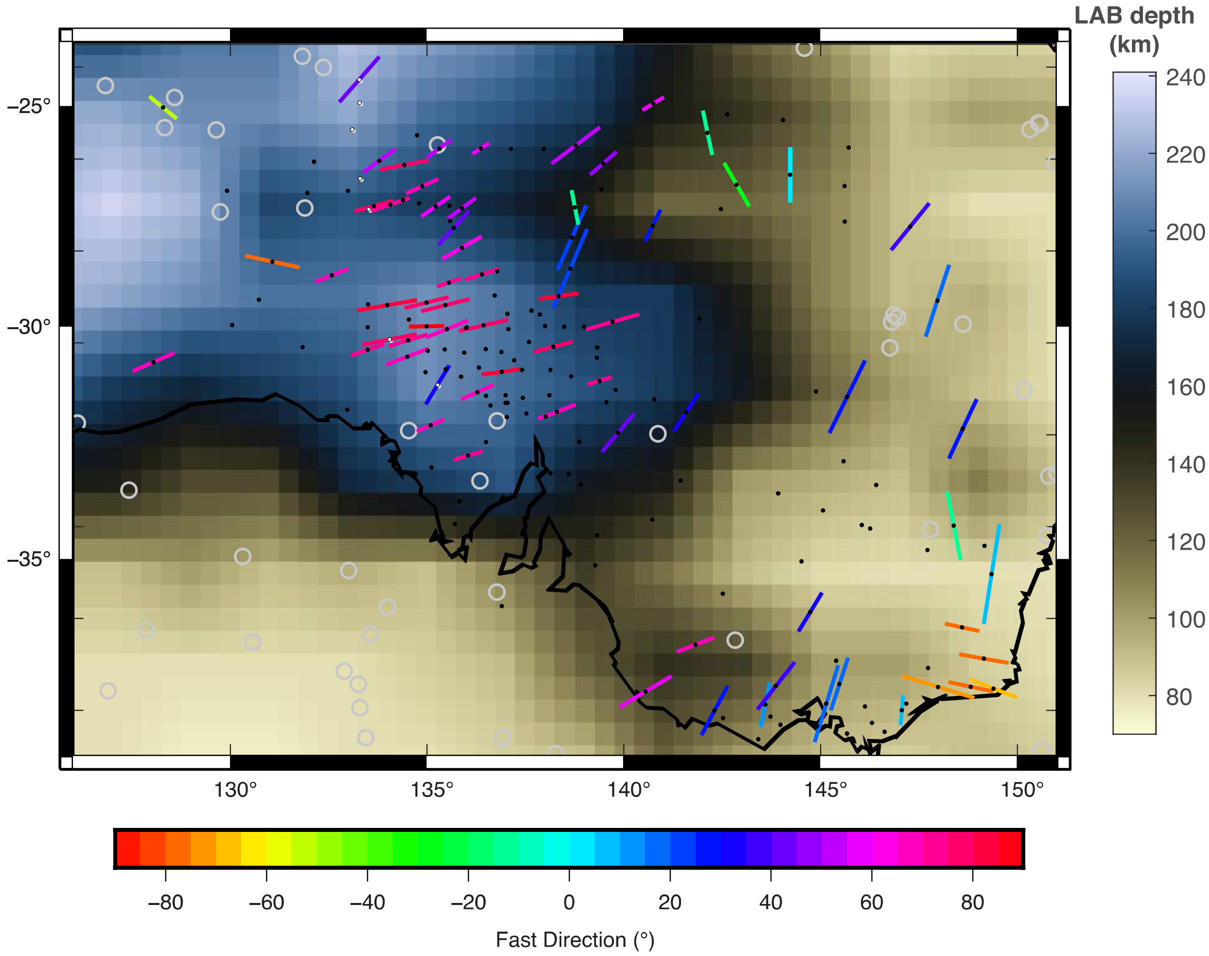

Figure S6. Comparison of stacked splitting results (same as Figure 3) with the location of Quasi-Love wave scatterers (grey open circles) from Eakin, (2021). Quasi-Love waves represent Love-to-Rayleigh wave scattering and are sensitive to lateral gradients in seismic anisotropy with peak sensitivity in the upper mantle ~ 100-200 km depth.

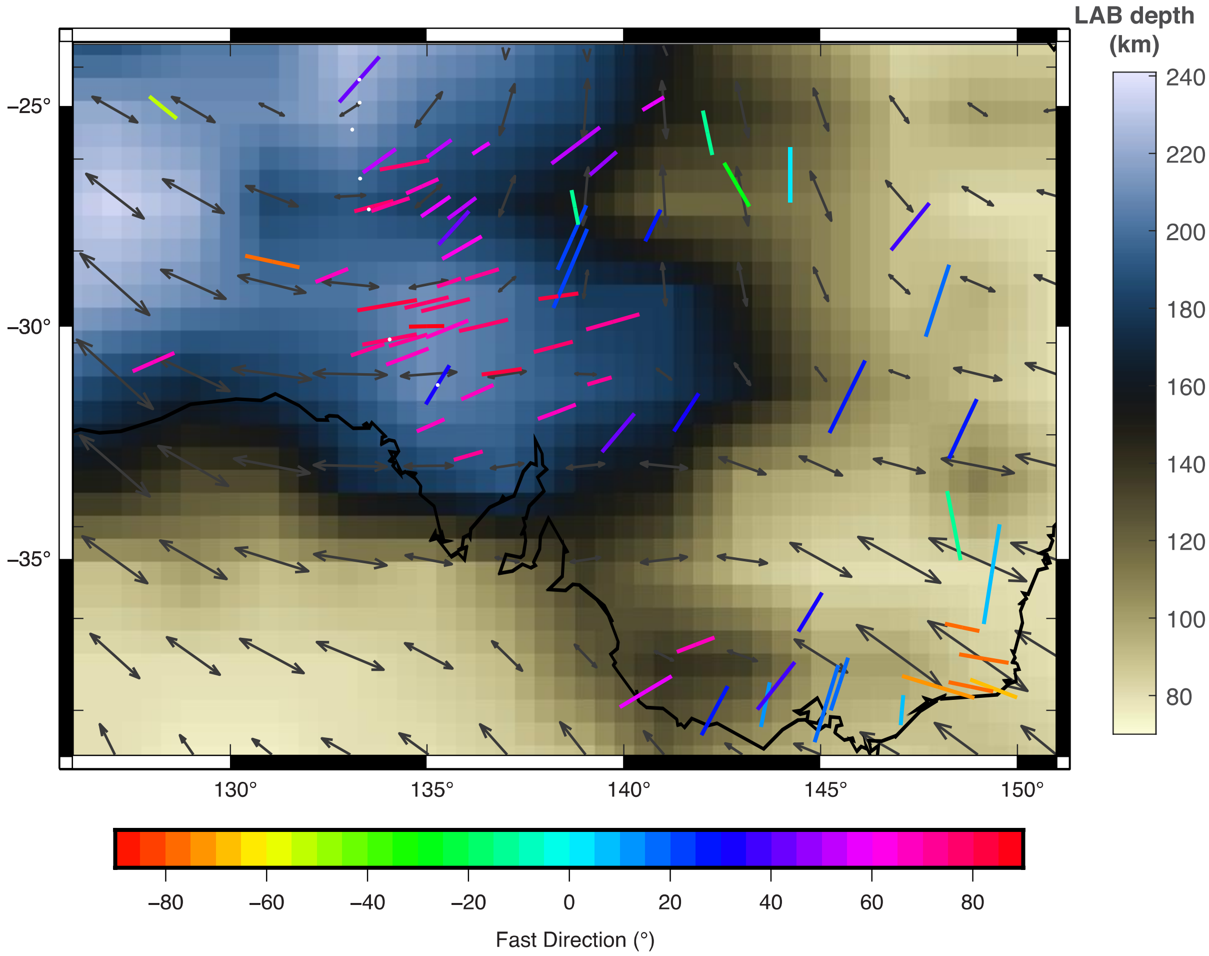

Figure S7. Comparison of stacked splitting results (same as Figure 3) with the pattern of surface wave derived azimuthal anisotropy at 50 km depth (grey arrows) from Debayle et al., (2016).

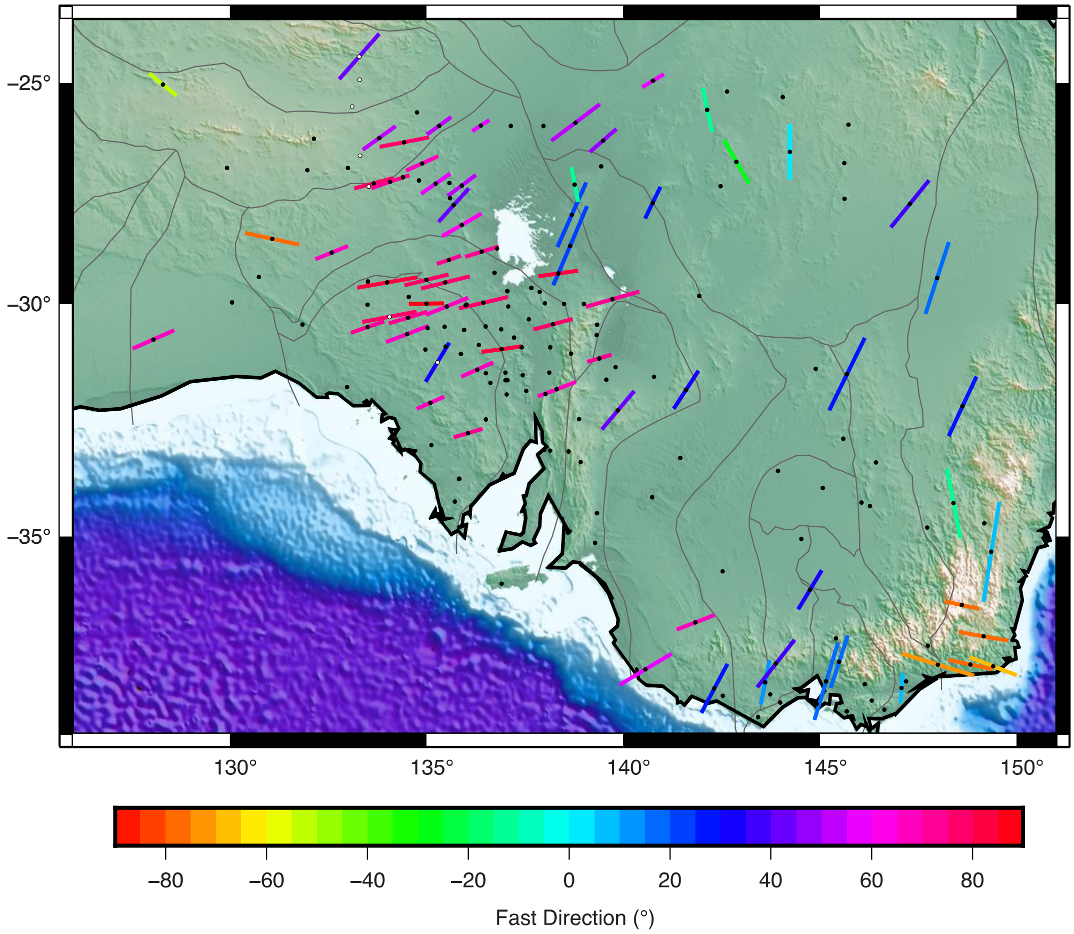

Figure S8. Comparison of stacked splitting results (same as Figure 3) with the crustal boundaries of Australia from Korsch and Doublier, (2015).

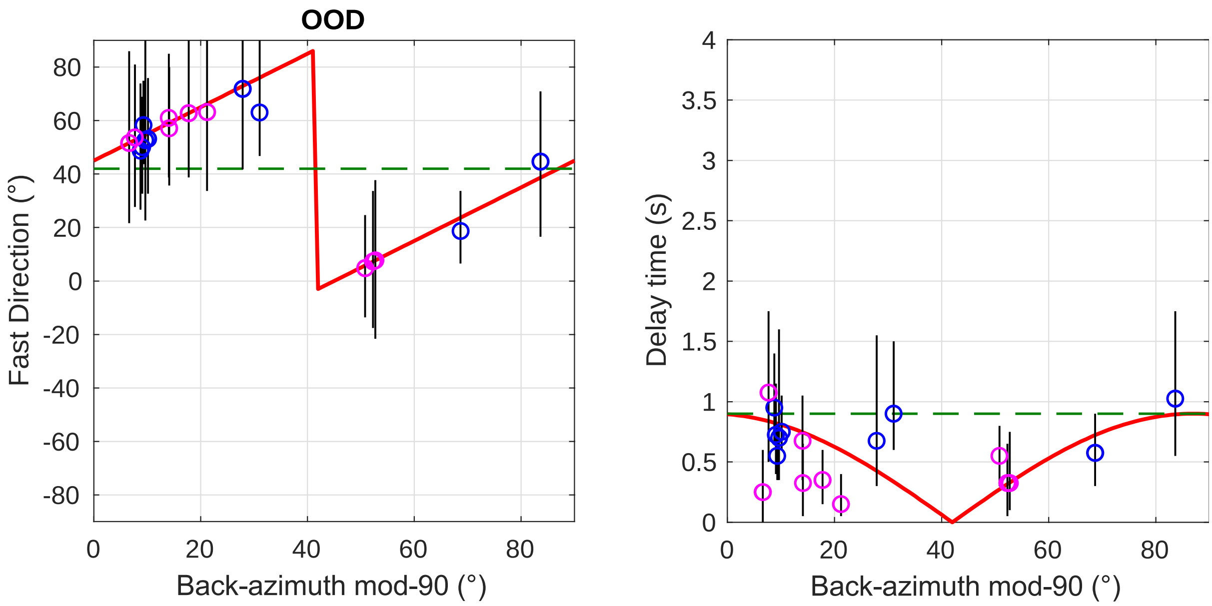

Figure S9. Retrieved splitting parameters (via the rotation correlation method) for station OOD from the Australian National Seismograph Network (AU) plotted as a function of event backazimuth (modulated over 90°). Results from SKS phases are plotted as blue circles, and PKS phases in magenta. The green dashed line represents the best-fit value for that station based on stacking of the individual error matrices (i.e. the values shown in Figure 3). The solid red line represents the predicted systematic error as a function of backazimuth, based on the stacked splitting parameter values (green), and the empirical equations from (Eakin et al., 2019). The systematic error prediction provides an excellent match to variation in splitting parameters with back-azimuth, especially the 45° slope in fast direction.

Figure S10 (below). Same as Figure S9 for all permanent AU stations that produced a stacked result, as shown in Figure 3.

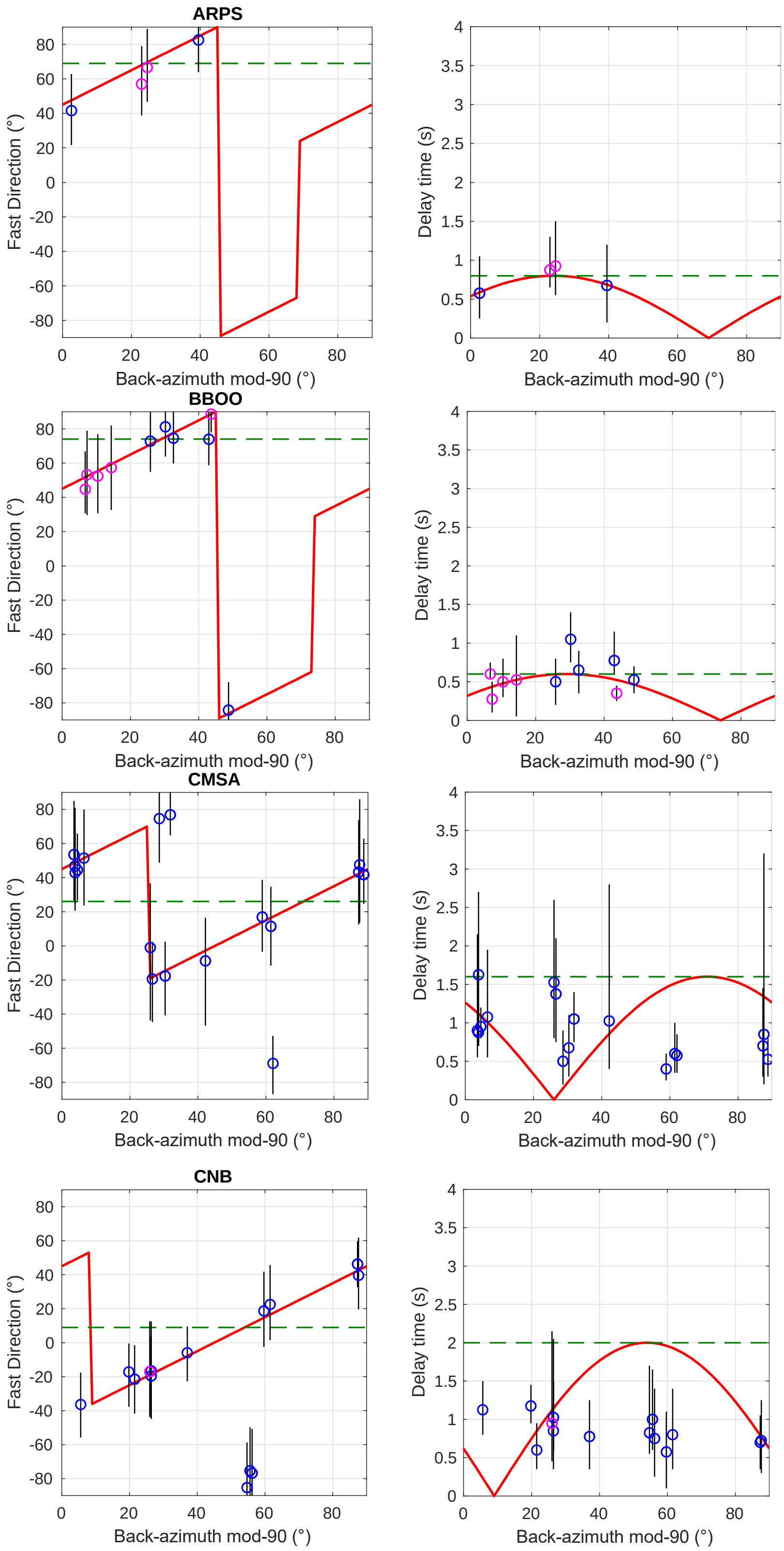

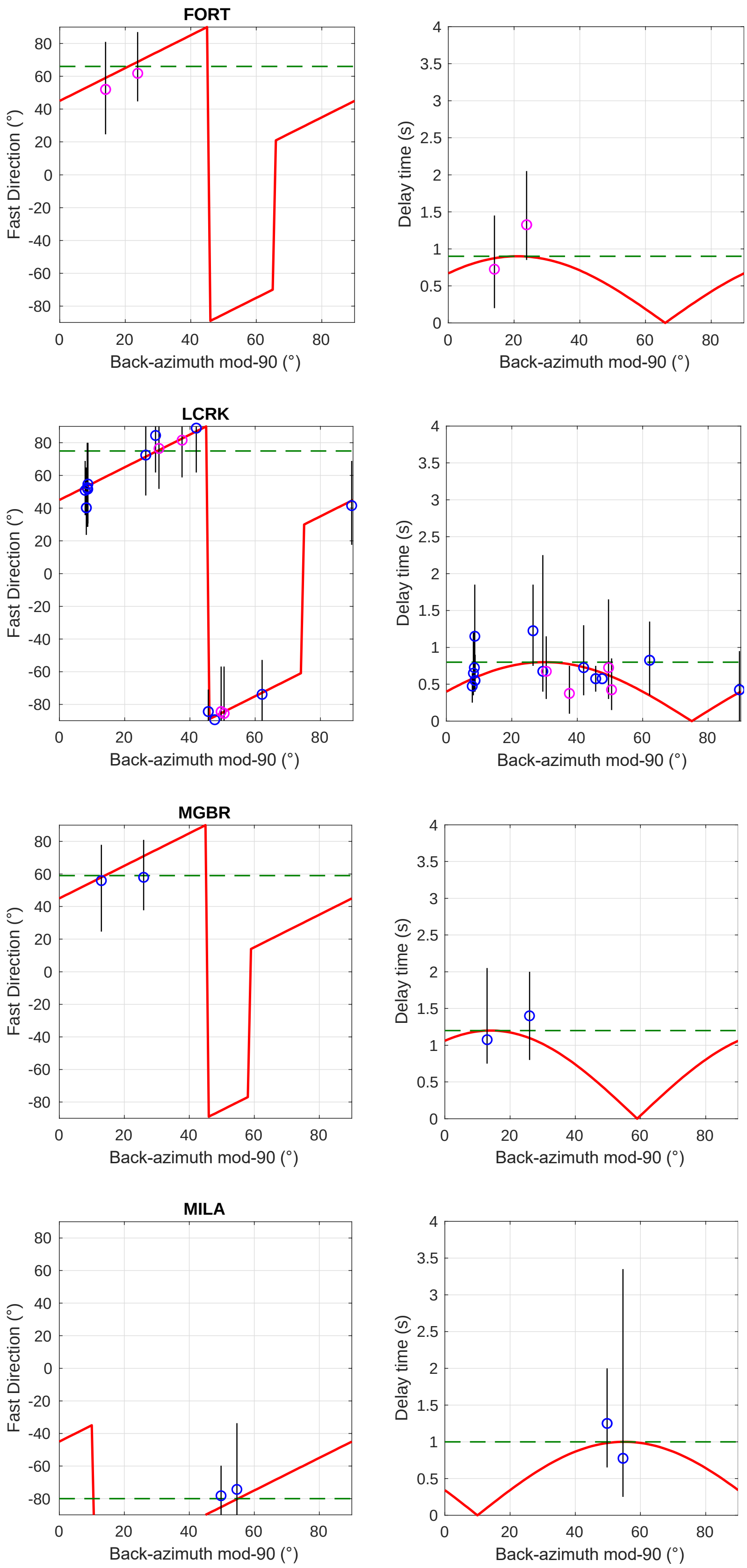
FORT
LCRK
MGBR
MILA
Fast Direction (°)
Delay time (s)
Back-azimuth mod-90 (°)

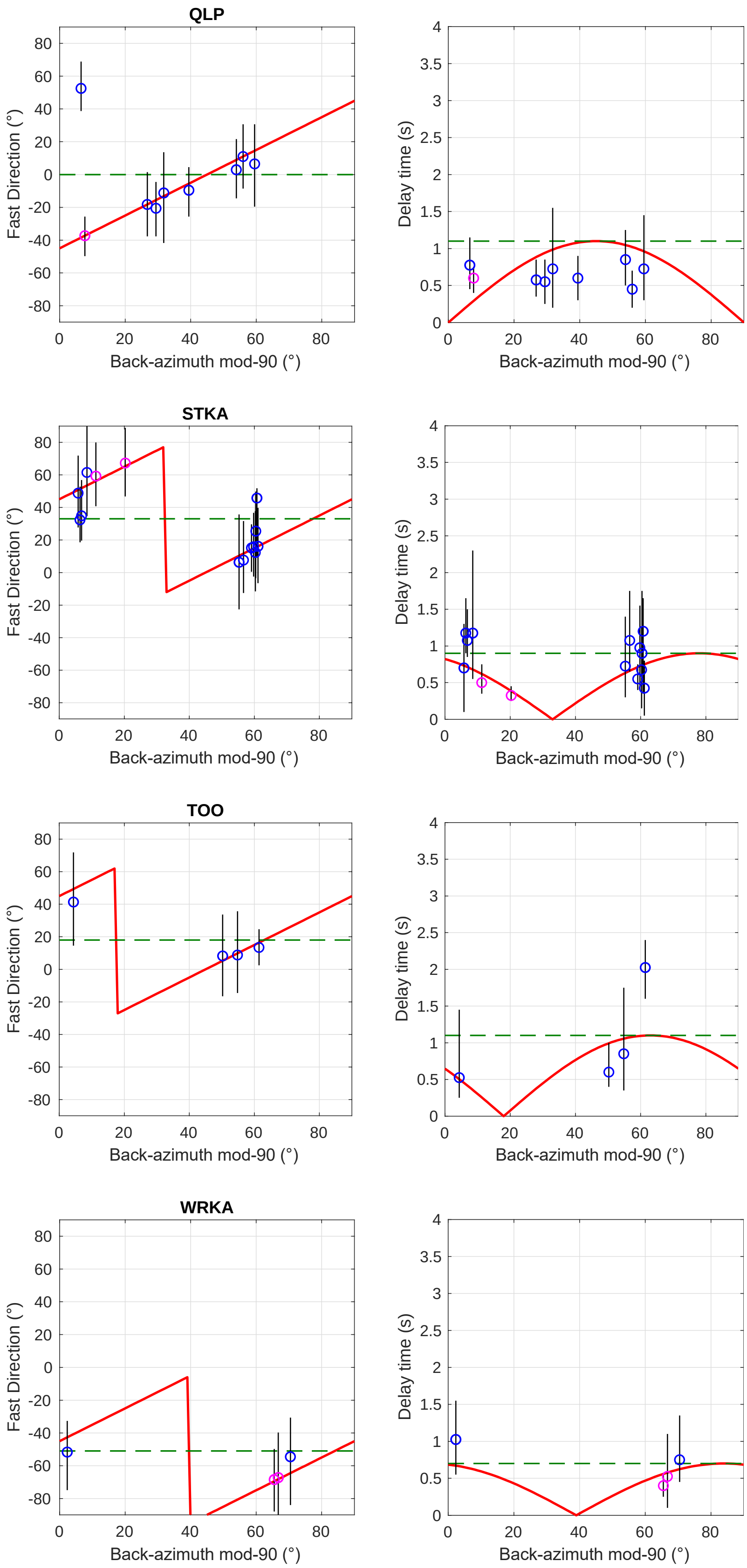
QLP
Fast Direction (°)
Back-azimuth mod-90 (°)
Delay time (s)
Back-azimuth mod-90 (°)
STKA
Fast Direction (°)
Back-azimuth mod-90 (°)
Delay time (s)
Back-azimuth mod-90 (°)
TOO
Fast Direction (°)
Back-azimuth mod-90 (°)
Delay time (s)
Back-azimuth mod-90 (°)
WRKA
Fast Direction (°)
Back-azimuth mod-90 (°)
Delay time (s)
Back-azimuth mod-90 (°)

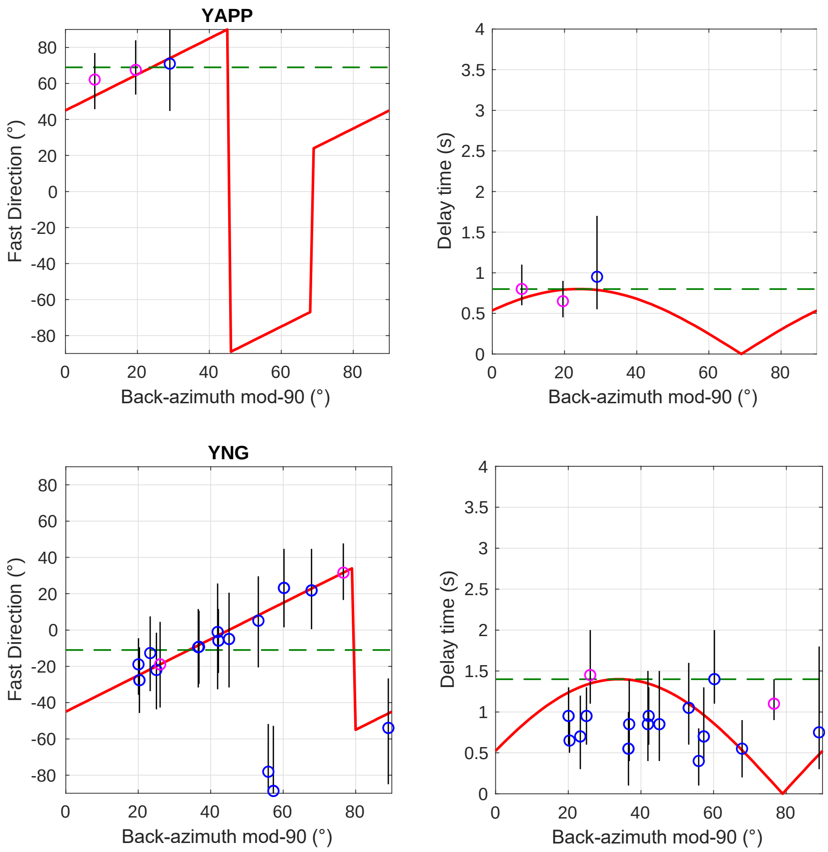

YAPP
Fast Direction (°)
Delay time (s)
Back-azimuth mod-90 (°)
YNG
Fast Direction (°)
Delay time (s)
Back-azimuth mod-90 (°)

Table S1: Excel spreadsheet containing list of individual measurements, and stacked shear wave splitting results for each station, found by this study.